Caving 2026 – A van As, D Cumming-Potvin & J Wesseloo (eds)

doi:10.36487/ACG_repo/2645_20

A flow-controlled support formulation for coupled cave propagation modelling

Yoann Hebert [a,*], Karl Lawrence [b], Bijan Peik [b]

[a] *Equilibrium Mining, Australia*

[b] *Equilibrium Mining, USA*

Abstract

Coupled continuum–flow simulations are widely used to simulate cave propagation, reflecting the influence of gravity-flow on stress redistribution and cave growth. While this influence is well recognised, how mobilised material interacts mechanically with the surrounding rock mass remains an open area of investigation; with a range of numerical formulations used in practice. This paper reviews existing coupled approaches with emphasis on how gravity flow is linked to stress redistribution. Building on this context, a new coupled formulation is introduced in which material mobilisation is represented through a controlled and progressive reduction in support and confinement at the cave boundary. The approach retains key physical mechanisms while improving computational efficiency for large-scale applications.

The methodology incorporates a dedicated gravity-flow formulation designed specifically for efficient coupling within large-scale three-dimensional cave simulations. The proposed formulation separates vertical support and lateral confinement mechanisms and introduces a locally defined propagation capacity that constrains cave growth based on flow activity and available void space. This provides a direct and physically consistent link between material movement and stress redistribution, while reducing sensitivity to coupling interval selection. The approach retains key physical mechanisms associated with cave propagation, including airgap development, overhang formation, cave stalling, and draw-strategy dependency, while remaining computationally practical for large-scale applications.

The methodology is demonstrated through a series of example applications, illustrating its ability to reproduce key cave propagation behaviours under different draw strategies and rock mass conditions.

Keywords: *cave propagation, numerical modelling, continuum–flow coupling*

1 Introduction

Cave mining relies on the controlled failure and gravity-driven mobilisation of large rock volumes, with cave propagation governed by stress redistribution in the surrounding rock mass. The evolution of the cave geometry, breakthrough timing, and associated geotechnical risks are strongly influenced by how stresses are redistributed as material within the cave mobilises and flows.

Observations and numerical studies have shown that gravity-driven material movement has a first-order influence on stress distribution around the cave, affecting confinement, load transfer, and the stability of the cave boundary (Beck et al. 2011; Fuenzalida et al. 2018; Hebert & Sharrock 2018). Numerical models that do not account for the mechanical influence of mobilised material may not reliably reproduce cave behaviour.

Coupled geomechanical–flow approaches have therefore been increasingly adopted to simulate cave propagation, allowing interaction between gravity-flow and rock mass response to be captured explicitly. A range of numerical formulations has been proposed, differing in numerical framework, rock mass

[*] Corresponding author. Email address: yhebert@equilibriummining.com

representation, and treatment of gravity-flow. While many of these approaches have demonstrated practical success, they can be computationally demanding for large-scale three-dimensional applications.

The key contribution of this work is a flow-controlled boundary formulation that links material mobilisation directly to support loss and cave propagation through a locally defined propagation capacity. This paper reviews key coupled geomechanical–flow approaches used for cave propagation modelling, with emphasis on how gravity-flow is linked to stress redistribution. Building on this context, a coupled formulation is proposed that differentiates internal cave mechanisms and represents their mechanical influence through a progressive reduction in support and confinement at the cave boundary, regulated by the locally allowable cave growth associated with material mobilisation. The approach retains key physical mechanisms while enabling computationally efficient simulation of three-dimensional cave propagation.

2 Review of existing coupled methodologies for cave propagation simulation

This section provides an overview of the modelling strategies that have been applied to cave propagation, with emphasis on the assumptions governing how material mobilisation modifies the stress field in the surrounding rock mass.

2.1 Cave propagation simulation without flow coupling

Continuum-based numerical methods have long been used to simulate cave propagation at the mine scale, primarily due to their ability to capture large-scale stress redistribution. An early attempt to simulate the caving process using FLAC3D was presented by Lorig (2000) as part of the International Caving Study (ICS), using a two-dimensional axisymmetric model in FLAC3D. In this approach, cave propagation was simulated by progressively reducing the vertical support at the undercut level, allowing caveability to be assessed based on the evolution of cave height. While this method provided a useful link to empirical caveability criteria, the resulting cave geometries were not representative of observed cave shapes (Hebert & Sharrock 2018).

A caving algorithm was developed as part of the International Caving Study (ICS I & II) and Mass Mining Technology projects (Board & Pierce 2009; Sainsbury 2012). It uses a production-driven formulation in which draw is represented through imposed velocities at the extraction level, enabling the simulated mass removal to match a defined draw schedule. In this framework, the imposed velocities control the rate of material extraction, while cave propagation emerges from the strain-softening response of the rock mass and the associated redistribution of stresses. This methodology has been widely used in mine scale cave modelling to date (e.g. Ghazvinian et al. 2020a).

The velocity-based formulation presents some challenges:

- Internal flow processes such as isolated draw, airgap formation, and rilling mechanisms are not explicitly captured and must be inferred through modelling assumptions, despite their recognised influence on cave behaviour and draw control (Fuenzalida et al. 2018).
- In practice, the use of imposed velocities requires sufficiently small values to avoid influencing the mechanical response, resulting in slow material collapse and long simulation times.

More recent work has introduced incremental improvements to this framework. Castro et al. (2024) incorporated the influence of airgap formation derived from a gravity-flow model, highlighting the importance of void development on cave behaviour and draw control. This reinforces the need to better integrate material flow with mechanical response, as discussed by Fuenzalida et al. (2018).

2.2 Gravity-flow formulations used in coupled cave propagation methods

Gravity-flow formulations are used to simulate the movement of fragmented material within the cave column as a function of draw, and are primarily applied to assess material migration, draw interaction, dilution, and airgap formation.

A range of modelling approaches have been developed to represent gravity-driven flow, including empirical, semi-empirical, and cellular automata-based formulations, which may incorporate deterministic or stochastic movement rules. Flow models that have been used in coupled flow–deformation simulations include:

- PCBC (Diering 2000): an empirical flow model based on relationships derived from physical modelling and operational data.
- REBOP/MASSFLOW (Pierce 2010): a semi-empirical model that incorporates rules based on mechanisms observed in PFC^{3D} simulations, small-scale physical model tests, and calibration to full-scale caving operations.
- CAVESIM (Sharrock et al. 2012; Hebert & Sharrock 2018): a lattice grain cellular automaton flow model that simulates gravity-driven movement of fragmented material using either a stochastic probabilistic transfer scheme or a Newtonian solver based on particle acceleration.
- FLOWSIM (Castro et al. 2018): a cellular automata-based model using probabilistic void-migration rules.

2.3 Coupling strategies between flow and mechanical response

Coupled cave propagation methods generally follow the same fundamental concept (Figure 1). The mechanical model resolves the stress field and defines the evolving cave geometry, with material classified as caved based on criteria such as strength degradation, displacement, or strain. This defines the volume available to flow. Production is then simulated within this domain using a gravity-flow model over a given time increment (typically weeks to months). The resulting flow metrics (e.g. movement zones, flow activity, airgap volume) are transferred back to the mechanical model, where they impact stress redistribution and subsequent cave growth. The process is repeated sequentially for the entire mining sequence.

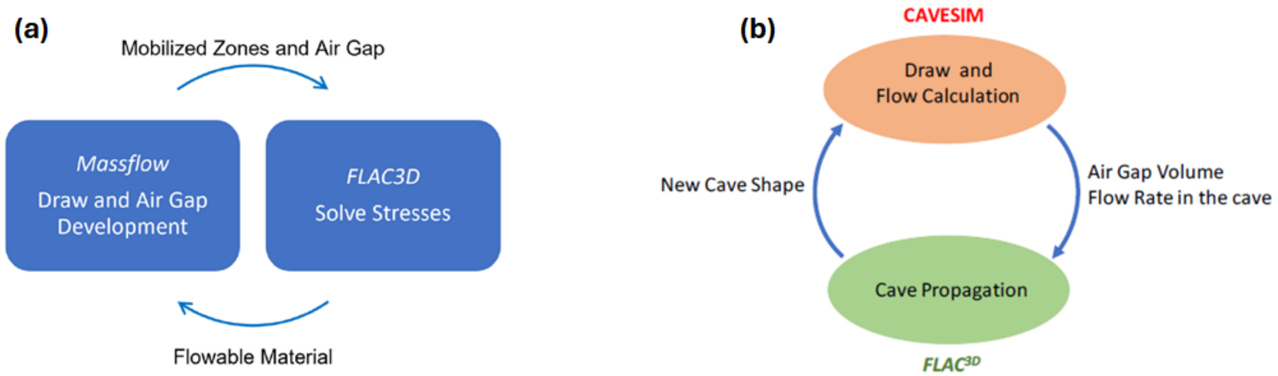

Figure 1 Conceptual illustration of bi-direction coupling methods to simulate cave propagation, after (a) Cancino et al. (2024) and (b) Hebert and Sharrock (2018)

Accurate representation of rock mass behaviour is fundamental to predicting cave propagation. This includes strain softening, strength degradation, dilation, bulking, and modulus reduction associated with the transition from intact rock to caved material. Several authors identify these mechanisms as critical to reproducing observed cave behaviour (e.g. Sainsbury 2012; Beck et al. 2011; Ghazvinian et al. 2020a; Hebert & Sharrock 2018). This topic is not the focus of the present paper, but it underpins all numerical methods. However, while the constitutive model governs how the rock mass responds to stress changes, it does not define how those stress changes are generated in response to flow.

A key challenge in coupled cave propagation modelling lies in representing the mechanical influence of the caved material on the surrounding rock mass. Gravity-flow models simulate material movement within the cave but do not provide direct estimates of stresses or forces within the muckpile, nor how these evolve during flow. As highlighted by Beck et al. (2011), this limitation requires the geomechanical model to approximate the mechanical effects of flow using surrogate measures derived from flow outputs. While considerable (and rightly so) attention is often given to the selection of constitutive models and material properties, the method used to translate material movement into stress changes largely controls the evolution of confinement and load transfer around the cave, and therefore the resulting cave propagation behaviour. Table 1 and Figure 2 summarise coupled algorithms reported in the literature, highlighting how information from the flow model is incorporated into the continuum model to represent the mechanical effects of flow.

Table 1 Summary of coupled methodologies and associated methods to simulate the impact of gravity-flow on the surrounding rock mass

Method	Modelling packages	Flow model output used	Mechanical representation in continuum model
Arndt et al. (2018)	ABAQUS + PCBC (Cellular Automata)	Airgap	Caved cells are assigned reduced ('soft') material properties in the finite element (FE) model, while airgap cells are set as stress-free.
Beck et al. (2011)	ABAQUS + CAVESIM	Flow velocity, Airgap	The discontinuum finite element (DFE) model updates the modulus of cave material as a function of flow state: mobile material is assigned a reduced transitional modulus, stationary cave material a higher modulus, and airgap zones are assigned near-zero stiffness (Figure 2d). The modulus evolves during coupling to represent changes in support conditions.
Castro et al. (2024)	FLAC3D + FLOWSIM	Airgap	Velocity-based continuum-only formulation (described in Section 2.1). Airgap volume nulled (void) in continuum model (Figure 2a).
Hebert & Sharrock (2018)	FLAC3D + CAVESIM	Flow velocity (volumetric flow rate), airgap	The continuum model applies a reduction in support pressure at the cave boundary. This is implemented as a local decrease in vertical stress at the cave boundary (within the cave), with the reduction factor defined as a function of volumetric flow rate (Figure 2c). Airgap zones are represented by further reducing this support.
Fuenzalida et al. (2018)	FLAC3D + MASSFLOW	Movement zones, airgap	All stress components are reset to zero within the movement zones while air regions are nulled (Figure 2b).

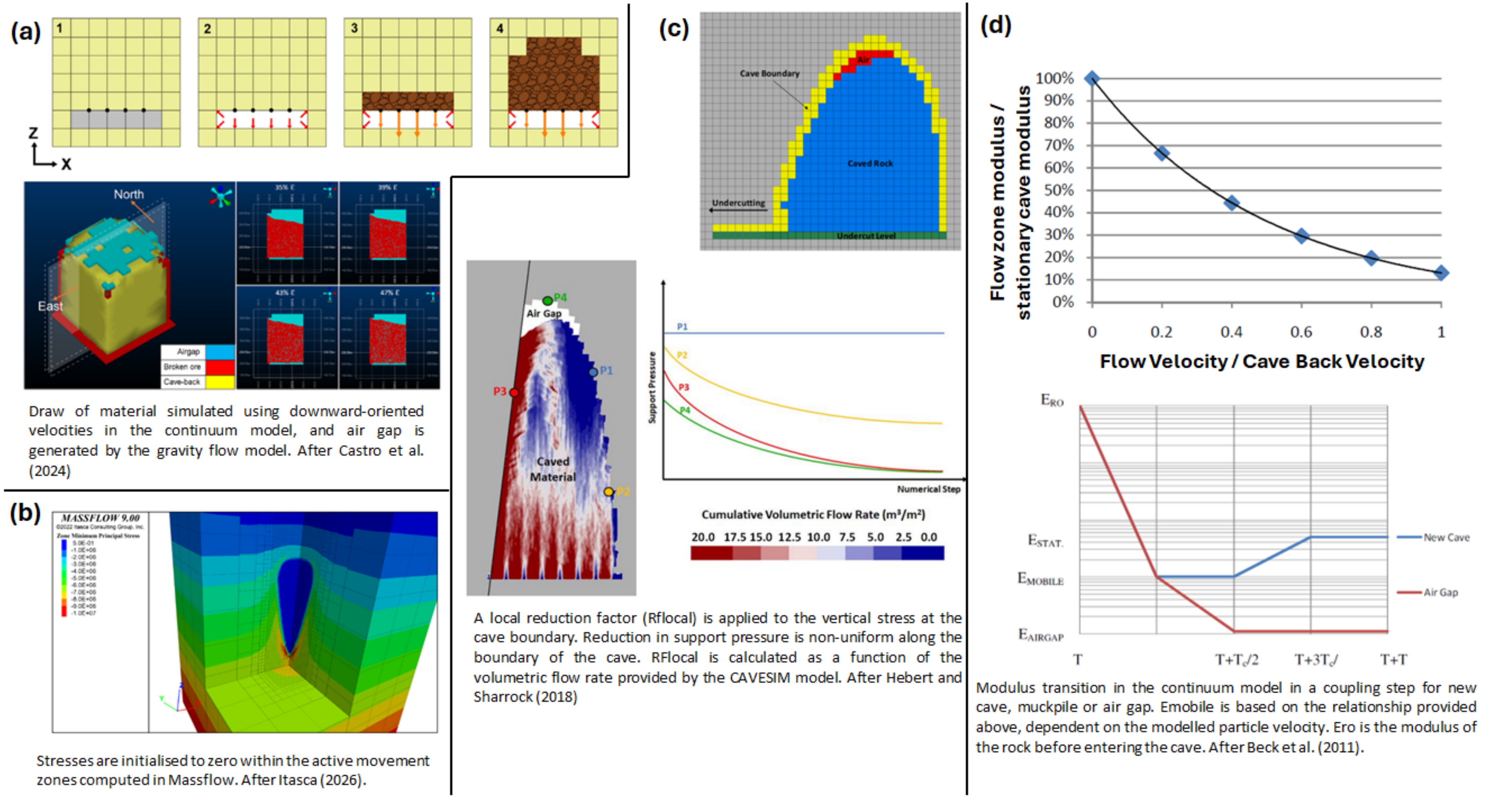

Figure 2 **Different methods used to represent the mechanical effects of flow in continuum cave models. Each method translates flow-model outputs into a modification of the continuum model, after (a) Castro et al. (2024), (b) Itasca (2026), (c) Hebert & Sharrock (2018) and (d) Beck et al. (2011)**

Across existing methodologies, interaction between flow and stress redistribution remains indirect and dependent on simplifying assumptions. One of the underlying reasons is the absence of a robust and validated framework to quantify the stress field within a flowing and fragmenting cave. Although concepts from granular mechanics, such as frictional arching and stress redistribution with depth, often described using Janssen-type formulations (describing stress arching and load transfer in granular silo systems), have informed the understanding of fragmented-rock behaviour, these are derived for confined, quasi-steady systems and are not directly applicable to the transient, three-dimensional and evolving conditions within a cave column. Pierce (2010) noted that the behaviour of caved rock differs from classical granular flow systems, with important differences in geometry, confinement, and the transient nature of material movement. More recent work has focused on estimating vertical stress within the broken column, demonstrating that it is controlled by local flow conditions, with load transfer from flowing regions to stagnant zones (Gómez & Castro 2022). In addition, stresses within the caved material are inherently transient and evolve continuously with material movement, whereas continuum models typically solve a sequence of quasi-static equilibrium states.

One limitation of existing approaches is that the mechanical influence of the caved material is often treated in a spatially uniform manner across the cave, without distinguishing between different support mechanisms. Vertical support is controlled by contact between the muckpile and the cave back and is highly sensitive to material mobilisation and airgap development. In contrast, lateral confinement is governed by arching and stress redistribution within the fragmented material and can persist during ongoing flow (e.g. Janssen 1895; Pierce 2010).

2.4 Coupling intervals and simulation of cave propagation in a quasi-static framework

In coupled cave propagation models, time is not simulated explicitly. Instead, it is tracked as a function of material extraction within the flow model (Hebert & Sharrock 2018). The simulation proceeds in discrete coupling intervals (typically weekly to monthly), with communication between the flow and geomechanical models occurring at the end of each period.

This assumption has important implications for the representation of cave propagation and is illustrated with a simple experiment in Figure 3. Consider a cave with an airgap of variable height along its span (Figure 3b). In reality, as material collapses and flows, regions with smaller airgap are filled earlier, leading to the progressive re-establishment of support from the muckpile and a local reduction in span. In contrast, regions with larger airgap may continue to propagate until sufficient material has collapsed to fill the entire void, or until the cave span becomes too small to sustain further growth (Figure 3d).

Accurately representing this process requires sufficiently small coupling intervals (e.g. days) to approximate the progressive filling of material within the cave. However, reducing the coupling interval increases computational cost. Larger intervals can lead to unrealistic cave shapes (Figure 3c), as the progressive filling of void is not resolved and the cave may artificially propagate over the full extent of the available void space within a single update.

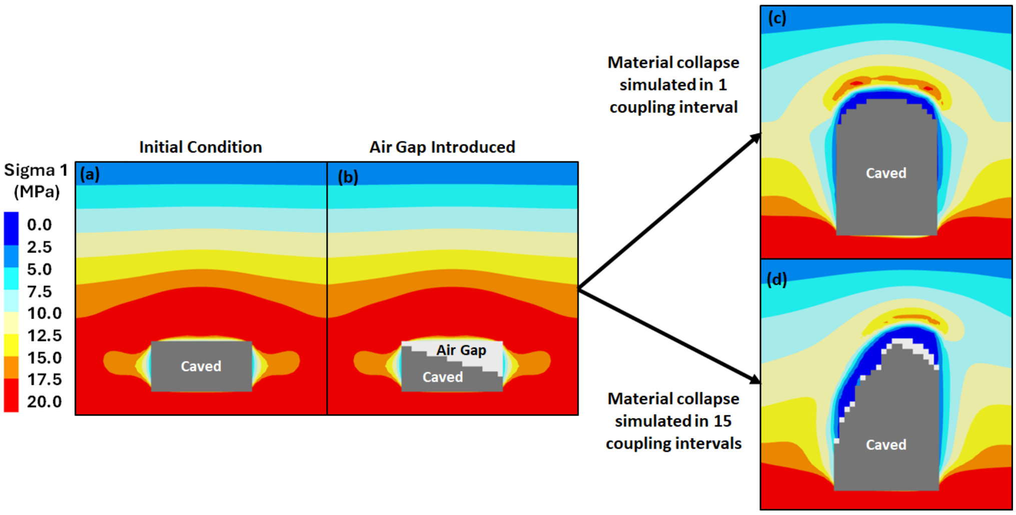

Figure 3 Illustration of the influence of coupling interval on simulated cave propagation. (a) Initial condition; (b) Introduction of an airgap of variable height along the cave span; (c) Cave response simulated over a single large coupling interval where cave propagation continues until sufficient material has caved to fill the entire airgap, after which the caved material is allowed to move into the void; (d) Cave response simulated using multiple smaller coupling intervals, allowing progressive collapse, partial filling of the airgap, and local re-establishment of support during cave propagation

Coupled cave propagation models are computationally demanding and time-consuming to calibrate and run (Beck et al. 2011; Arndt et al. 2018). The requirement for small coupling intervals contributes significantly to this, combined with the need to simulate cave propagation over extended production periods. For example, 100 years of production in a large multi-cave operation would result in 5,200 coupling intervals when using weekly increments, representing a significant computational burden.

3 Proposed coupled formulation for cave propagation

The approach proposed in this paper builds on existing coupled continuum–flow methodologies and introduces an alternative representation of the mechanical effect of gravity-flow within the continuum model. The formulation is based on 3 primary objectives:

1. To provide a physically meaningful representation of the influence of material movement on stress redistribution and cave propagation.
2. To reduce coupling interval dependency in cave propagation modelling.
3. To improve computational efficiency, enabling practical simulation of large-scale and multi-cave systems.

3.1 Constitutive model

Within a continuum framework, the constitutive model defines the response of the rock mass to loading and failure. A strain-softening formulation is adopted to represent progressive degradation from peak to residual strength, consistent with established industry practice for large-scale geomechanical modelling (e.g. Ghazvinian et al. 2020b; Hebert & Sharrock 2018; Sainsbury 2012).

Peak strength is defined using the Hoek–Brown failure criterion, implemented through a stress-dependent Mohr–Coulomb approximation, with post-peak behaviour governed by accumulated plastic shear strain. The formulation incorporates modulus softening, dilation, and brittleness controls, enabling progressive damage development and stress redistribution as yielding occurs.

3.2 Gravity-flow code

A range of commercially available gravity-flow codes exists to simulate material movement inside the cave. The list provided in Section 2.2 is not comprehensive and only refers to codes previously used for coupling. These tools are typically designed to provide estimates of grade recovery, dilution, fragmentation, and fines migration, and can represent flow behaviour in significant detail. In the context of coupled cave propagation modelling, however, the role of the flow model is fundamentally different. As discussed in Section 2.3, the mechanical influence of material movement is not transferred directly as stresses but is instead approximated within the continuum model. Consequently, increasing the level of detail in the flow simulation does not necessarily lead to a more accurate representation of stress redistribution or cave propagation.

The gravity-flow code developed as part of this work is intentionally simplified and designed specifically for integration within a coupled caving framework. It is based on a stochastic cellular automata formulation and is intended to reproduce the key characteristics of material movement within the cave (movement zones, interactive draw, bulking, airgap formation, rilling mechanisms, angle of repose on free surface), without explicitly modelling processes such as grade recovery, dilution, or fines migration. Stochastic cellular automata methods have been widely applied to simulate gravity-driven flow in caving operations and are well documented in the literature (Sharrock et al. 2012; Gibson 2014; Power & Campbell 2016; Castro et al. 2018). By focusing only on the mechanisms required for coupling, the model retains a physically meaningful representation of material movement while remaining computationally efficient.

The gravity-flow model is also designed to be highly efficient and scalable for large-scale multi-cave systems. To achieve this, the simulation domain is discretised into a three-dimensional voxel grid underpinned by chunked sparse data structures, ensuring that calculations are confined exclusively to regions containing active voids generated during material extraction. Active chunks and voids are tracked and updated dynamically as the simulation evolves, meaning computational cost scales with the number of actively flowing cells rather than the size of the cave or model domain. This implementation reduces dynamic memory allocation and mitigates cache inefficiencies typically associated with large contiguous data arrays. While gravity-flow calculations are not typically the primary computational bottleneck in a coupled framework, in the authors' experience, they can represent 10 to 20% of total run time depending on the implementation. The implementation described above reduces this contribution to less than 1% for the example applications considered in this paper.

3.3 Impact of flow on mechanical response

The proposed formulation is based on 3 key concepts used to represent the mechanical influence of flow on cave propagation.

1. The mechanical response of the caved material is not modelled explicitly. As discussed in Section 2.3, stresses within the flowing caved material are inherently approximated in a continuum framework. In the present approach, the support provided by the muckpile to the cave back and sidewalls is therefore represented as a boundary condition through equivalent forces applied at the cave–rock interface. This provides a direct and computationally efficient representation of the interaction between material movement and the surrounding rock mass. Because stresses within the cave do not need to be resolved explicitly during cave propagation, computational effort decreases progressively as the cave grows.
2. The mechanical support provided by the caved material is separated into 2 distinct mechanisms: vertical support at the cave back and lateral confinement along the cave sidewalls. These components are treated independently within the formulation to reflect their different roles in load transfer and their distinct response to flow (as discussed in Section 2.3).
3. The formulation introduces a locally defined propagation capacity, which constrains the allowable extent of cave growth based on flow conditions and available void space. Cave propagation is explicitly limited by the capacity of the system to accommodate bulking and material mobilisation.

This capacity is evaluated locally along the cave boundary, based on both flow activity and the available void space within the cave (airgap). By limiting propagation in this way, the formulation reduces dependency on the chosen coupling interval and provides a more direct link between flow-driven material movement and mechanically simulated cave growth.

The practical implementation of the formulation follows the following steps (illustrated in Figure 4):

- Stage 1: reference equilibrium state – the cave geometry is defined as the mobilised zone and the system is brought to equilibrium assuming the cave provides full mechanical support to the surrounding rock mass (Figure 4a). At this stage, the cave is treated as fully filled with caved material, irrespective of the presence of airgaps, in order to establish the reference stress state and the maximum support condition provided by the muckpile at the cave boundary. At the start of the simulation, the cave is defined by the initial undercut volume.
- Stage 2: application of equivalent reaction forces – the cave is converted to null material, and equivalent reaction forces are applied at the cave–rock interface to reproduce the support provided by the muckpile in the reference state (Figure 4b).
- Stage 3: classification of support mechanisms: the reaction forces are partitioned into 2 categories – vertical support forces acting on the cave back, and lateral confinement forces associated with arching of the muckpile against the cave sidewalls (Figure 4b).
- Stage 4: flow update and evaluation of local response – a production increment is simulated in the flow model. Flow activity and airgap distribution are evaluated in the vicinity of the cave boundary. For gridpoints/nodes associated with vertical support, a maximum allowable boundary velocity is calculated locally based on flow activity or airgap size, providing a measure of allowable cave propagation at that location. For gridpoints associated with lateral confinement (arching), a target reduction in confinement is defined as a function of flow activity.
- Stage 5: progressive reduction of boundary support – reaction forces are updated progressively from the reference state toward the flow-controlled state (Figure 4c). Lateral confinement forces are reduced linearly toward the target confinement defined from flow activity. Vertical support forces are reduced as a function of boundary velocity: when grid point velocities are low relative to the allowable value, support is reduced more aggressively; as velocities approach the maximum allowable velocity, the rate of reduction decreases. This ensures a stable and controlled transition while enforcing the local propagation capacity. By limiting propagation in this way, the formulation reduces dependency on the chosen coupling interval by constraining cave growth to remain consistent with the local capacity of the system to accommodate mobilisation and bulking.
- Stage 6: mass balance and propagation control – as boundary support is reduced, stresses redistribute around the cave, leading to yielding, softening, and displacement of the surrounding rock mass. The evolving cave volume is monitored relative to the maximum admissible volume defined from draw and bulking. Cave propagation continues until this propagation limit is reached, or until further cave growth ceases due to stalled conditions.
- Stage 7: geometry update and iteration – newly caved zones are identified, and an updated cave geometry is defined based on the extent of mobilised material (Figure 4d). This updated cave shape is then passed to the flow model, where material is allowed to move within the revised domain, and the process is repeated from Stage 1 for the next coupling step.

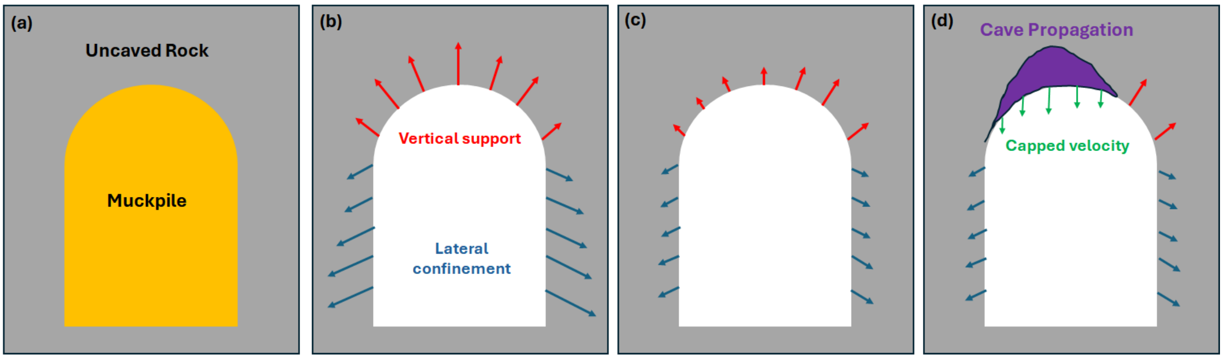

Figure 4 Schematic implementation of the formulation. (a) Initial equilibrium with a full cave; (b) Application and categorisation of equivalent forces; (c) Progressive reduction of boundary support informed by flow activity; (d) Cave propagation

In practice, additional numerical controls can be incorporated to improve computational efficiency during long-term simulations. These may include adaptive coupling intervals, criteria to identify stalled cave conditions, or adjustment of solution controls during periods of slow cave propagation. While such strategies have been implemented within the current framework and can significantly reduce overall simulation time, their detailed treatment is beyond the scope of the present paper.

4 Example application

A coupled cave propagation model should be able to capture key aspects of caveability, including overhang formation, the influence of draw-strategy on cave propagation, the potential for cave stall, airgap development, timing of surface breakthrough or interaction with other lifts, crater development, and surface subsidence (Hebert & Sharrock 2018). Examples in this section are provided to demonstrate the ability of the proposed formulation to capture these mechanisms.

4.1 Example 1: influence of draw-strategy on cave propagation

The example presented in this section focuses on the influence of the draw-strategy on cave propagation. A single cave was considered with a 250 × 200 m footprint (Figure 5) located at a depth of 800 m. The rock mass is assumed to be homogeneous, with properties provided in Table 2. A strain-softening constitutive model is used to represent progressive strength degradation and damage, as described in Section 3.1. The cave is developed using an advance undercut strategy oriented subparallel to the short axis of the footprint. The undercut advances at a constant rate of 2,500 m² per month until the entire footprint is established.

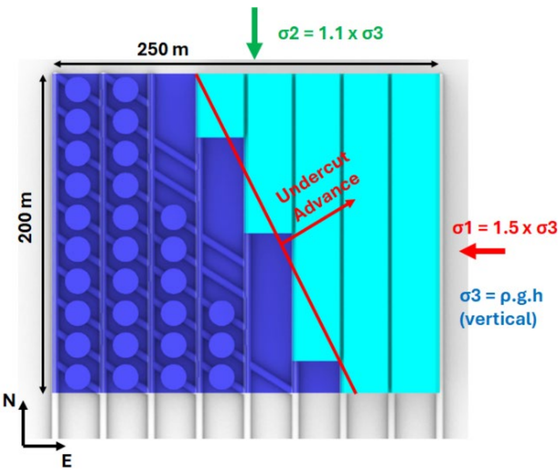

Figure 5 Plan view of footprint geometry, undercutting direction and pre-mining stress assumptions

Table 2 Adopted rock mass parameters

Rock mass parameter	Value
Intact modulus	15 GPa
Intact uniaxial compressive strength (UCS)	60 MPa
Geological strength index (GSI)	50
mi	12
Density	2,800 kg/m^3

Two draw strategies, illustrated in Figure 6 are considered to evaluate the influence of gravity-flow on cave propagation behaviour:

- The first strategy corresponds to a panel draw approach, characterised by an aggressive ramp-up during cave establishment. Production increases over a period of eight months to reach a target draw rate of 200 mm/day. Under this strategy, early drawpoints reach full production before completion of the undercut.
- The second strategy represents a block draw approach. A low and uniform draw rate of 50 mm/day is applied across the footprint until completion of the undercut. Following this, a 12-month rebalancing period is introduced, during which higher draw rates are applied to the most recently activated drawpoints to progressively even out the cave profile. After this period, a uniform draw rate of 200 mm/day is applied across the entire footprint.

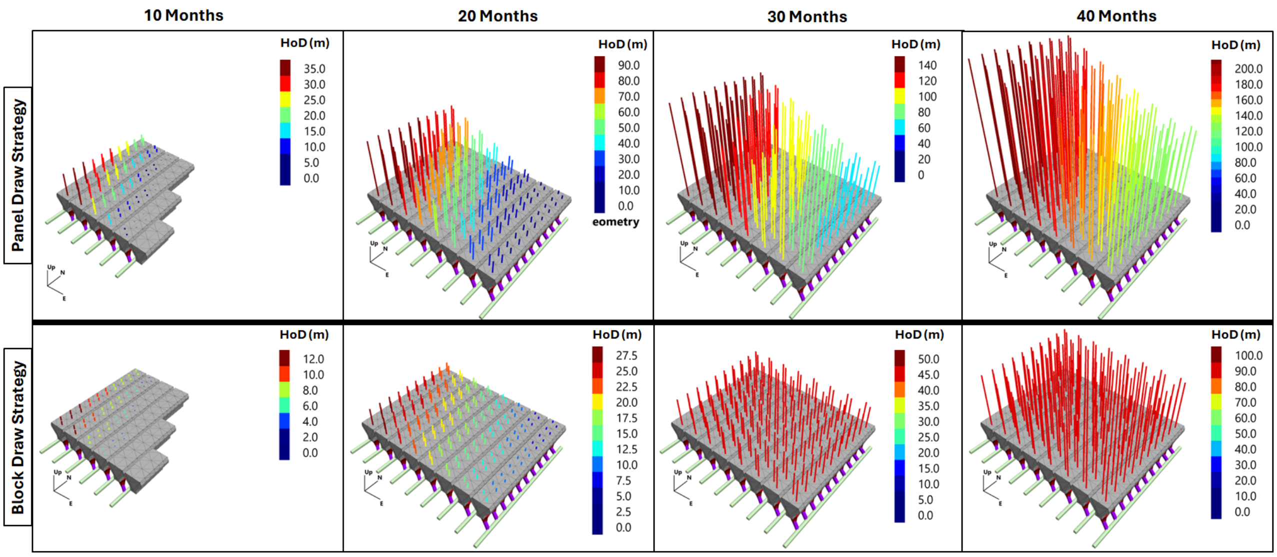

Figure 6 Height of draw over time for the 2 adopted draw strategies

The rock mass has been intentionally selected to be relatively weak with respect to the in situ stress field and cave span. Under these conditions, the cave is expected to propagate freely in response to draw. The objective of this example is to demonstrate the ability of the proposed formulation to properly capture the impact of different draw strategies on cave propagation behaviour.

The simulated cave shapes and flow activity (volumetric flow rate) for these 2 draw strategies are illustrated in Figures 7 and 8. The results indicate that, under identical rock mass and stress conditions, the cave response is strongly influenced by the draw-strategy. Panel draw promotes early cave propagation in the southwest corner of the footprint, the formation of a relatively narrow cave back, and early surface breakthrough (Figure 7). In contrast, the block draw-strategy delays cave propagation and results in the formation of a much broader cave back (Figure 8). Although both strategies ultimately reach similar production levels, the timing and geometry of cave propagation differ significantly. This highlights the sensitivity of cave behaviour to draw-strategy and demonstrates that the proposed formulation can translate gravity-flow into distinct cave propagation responses.

The small air pockets shown locally along the steep advancing face of the cave are a numerical mapping artefact. They occur where the jagged cave boundary geometry (associated with mesh discretisation) results in small local air pockets along the cave boundary (typically 2–3 cells in the flow model at a 2 m cell size). During mapping, a FLAC3D zone is classified as air when more than 20% of the embedded flow cells within that zone are air. These features are not interpreted as mechanically significant airgaps.

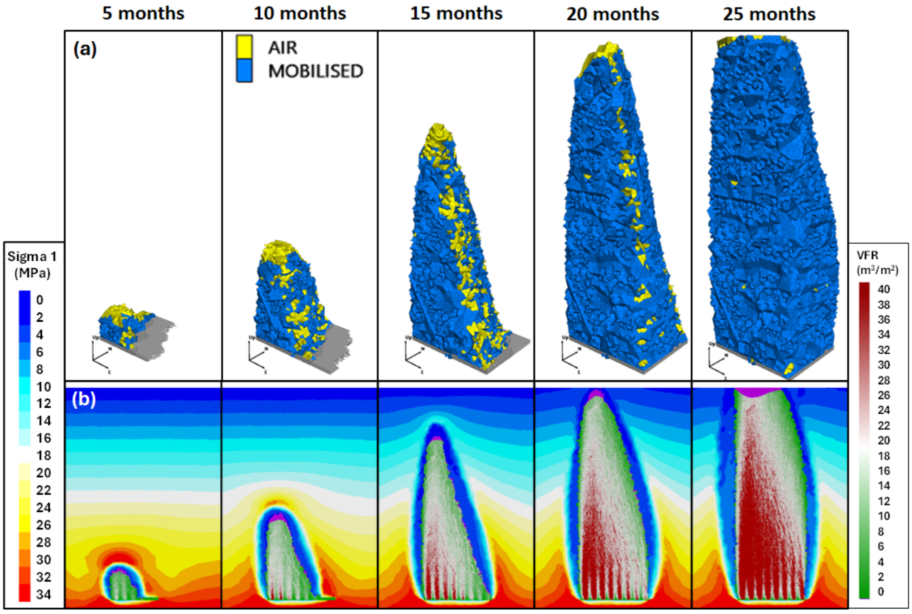

Figure 7 Cave propagation to surface simulated with the panel draw-strategy in weak rock. (a) Cave shape (mobilised zone); (b) East–west section through the centre of the footprint of flow activity within the cave (volumetric flow rate) and major principal stress in the surrounding rock mass

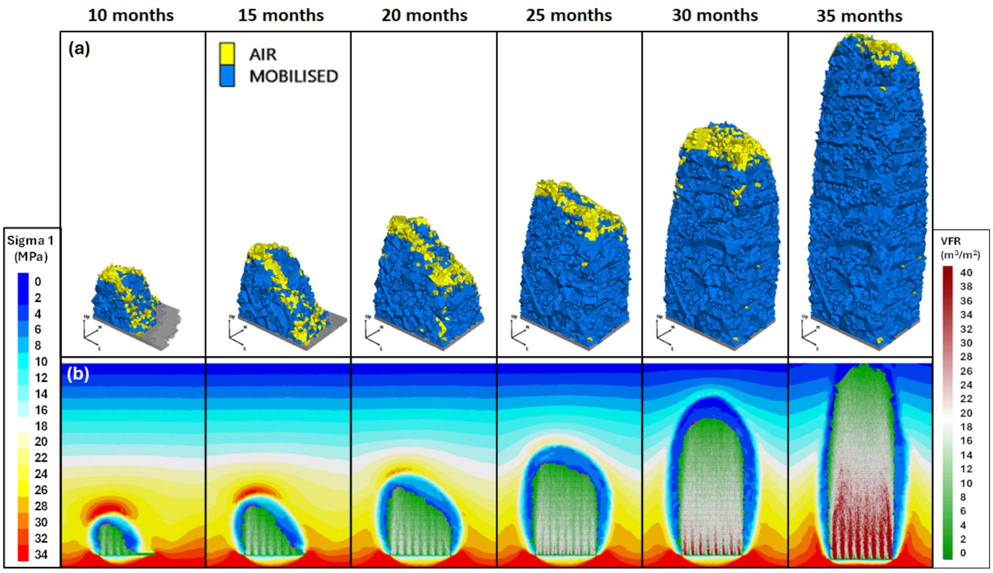

Figure 8 Cave propagation to surface simulated with the block draw-strategy in weak rock. (a) Cave shape (mobilised zone); (b) East–west section through the centre of the footprint of flow activity within the cave (volumetric flow rate) and major principal stress in the surrounding rock mass

One way to assess the model response is to compare the simulated cave geometry with the theoretical cave height derived from the height of draw at each drawpoint and bulking factor, using Equation (1). If the cave propagates freely in response to draw, the simulated cave height should match the theoretical value.

$$H_{Cave} = \frac{HoD}{1 - \frac{1}{BF}} \tag{1}$$

where:

H_{cave} = theoretical height of the cave above a drawpoint

HoD = drawpoint height of draw

BF = bulking factor (110% in this example).

Figure 10 compares the simulated cave geometry with the theoretical cave height (displayed in red lines) for both draw strategies. A good agreement is observed, indicating that cave propagation in the model is primarily controlled by draw and bulking under these conditions. This also confirms that the proposed implementation can correctly reproduce the expected cave response to draw.

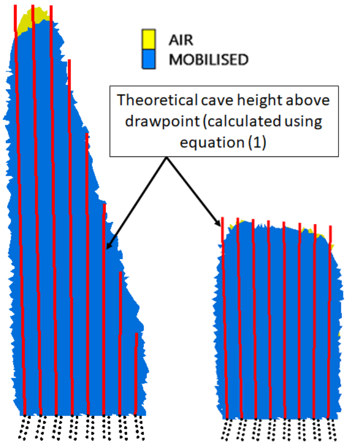

Figure 10 Simulated cave height versus theoretical, panel draw (left) and block draw (right)

4.2 Example 2: overhang formation and cave stalling

The second example considers the same mine geometry and panel draw-strategy as described in Section 4.1, but in a stronger rock mass (UCS 100 MPa, GSI 65, mi 18). The objective of this example is to demonstrate the ability of the formulation to reproduce key cave propagation mechanisms associated with poor caveability, including overhang formation, cave stalling, and airgap development.

Figure 11 illustrates the evolution of the cave in an east–west cross-section through the centre of the footprint. A slight overhang develops early on the western side of the footprint, leading to a localised increase in draw concentration in this area, as evidenced by higher volumetric flow rates. At the end of undercutting, a stable 73° overhang develops on the east side of the footprint. Material rilling along the overhang is observed. The overhang progressively reduces the span of the cave crown as it propagates. Halfway through the column, cave propagation becomes intermittent due to the reduced span available in a lower stress environment. The cave eventually stalls, and a large airgap (approximately 150 m high) develops.

Note that no faults have been included in this example, to provide a clearer understanding of the model response. In practice, faults are a key controlling factor and can significantly influence cave propagation, especially in strong rock environments.

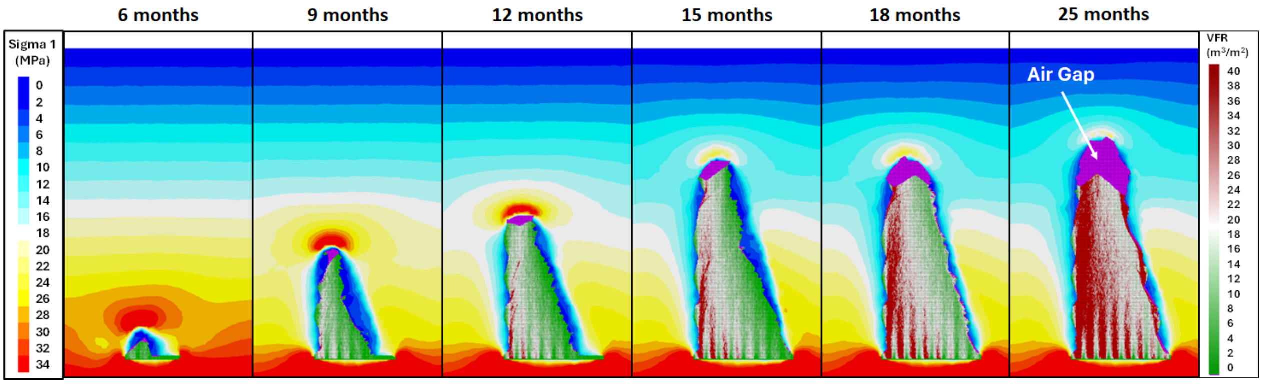

Figure 11 Cave propagation in stronger rock. East–west section through the centre of the footprint of flow activity within the cave (volumetric flow rate) and major principal stress in the surrounding rock mass

5 Limitations

The proposed formulation provides a new direction for coupled cave propagation modelling, highlighting an alternative way to represent the mechanical influence of flow within a continuum framework. Further work is required to refine the representation of support mechanisms, assess sensitivity to key parameters, and validate the method against operational data. More broadly, the formulation highlights the need for improved understanding and quantification of stress distribution within actively flowing caves. It is hoped that this work contributes to ongoing efforts in this area and encourages further research into the mechanical behaviour of fragmented material under caving conditions.

6 Conclusion

A new coupled formulation has been proposed in which the mechanical influence of caved material is represented through boundary conditions applied at the cave–rock interface. The approach separates vertical support and lateral confinement mechanisms and introduces a locally defined propagation capacity that constrains cave growth based on flow activity and available void space. This formulation provides a direct and physically consistent link between material movement and stress redistribution, while reducing sensitivity to coupling interval selection.

The proposed approach builds on established coupled cave propagation methodologies while introducing an alternative representation of flow-induced support loss within a continuum framework. The methodology retains key physical mechanisms associated with cave propagation, including airgap development, overhang formation, draw-strategy dependency, and cave stalling, while remaining computationally practical for large-scale three-dimensional applications.

Further work is required to refine the representation of support mechanisms, assess sensitivity to key parameters, and validate the methodology against operational datasets. More broadly, the formulation highlights the need for improved understanding and quantification of stress redistribution within actively flowing caves.

References

Arndt, S, Bui, T, Diering, T, Austen, I & Hocking, R 2018, 'Integrated simulation and optimisation tools for production scheduling using finite element analysis caving geomechanics simulation coupled with 3D cellular automata', *Caving 2018: Proceedings of the International Symposium on Block and Sublevel Caving*, Australian Centre for Geomechanics, Perth, pp. 247–258, https://doi.org/10.36487/ACG_rep/1815_16_Arndt

Beck, D, Sharrock, G & Capes, G 2011, 'A coupled DFE–Newtonian cellular automata scheme for simulation of cave initiation, propagation and induced seismicity', in *Proceedings of the 45th US Rock Mechanics/Geomechanics Symposium*, American Rock Mechanics Association, Eaton.

Board, M & Pierce, M 2009, 'A review of recent experience in modelling of caving', *Proceedings of the International Workshop on Numerical Modelling for Underground Mine Excavation Design, in conjunction with the 43rd US Rock Mechanics Symposium*, NIOSH Pittsburgh Research Laboratory, Bruceton.

Cancino, C, Fuenzalida, M & Kamp, C 2024, 'Numerical modeling of cave propagation and breakthrough timing', in Daniel Johansson & Håkan Schunnesson (eds), *MassMin 2024: Proceedings of the International Conference & Exhibition on Mass Mining*, Luleå University of Technology, Luleå, pp. 548–568, https://doi.org/10.36487/ACG_repo/2435_D-07

Castro, R, Oyarzo, D, Gómez, R, Suzuki, K & Cifuentes, M 2024, 'Coupling geomechanical and gravity flow models to obtain more representative flow simulations and air-gap risk identification in caving mining', *International Journal for Numerical and Analytical Methods in Geomechanics*, vol. 49, pp. 376–390, https://doi.org/10.1002/nag.3880

Castro, R, Arancibia, L, Guzman, D & Henriquez, JP 2018, 'Experiments and simulation of gravity flow in block caving through FlowSim', in Y Potvin & J Jakubec (eds), *Caving 2018: Proceedings of the Fourth International Symposium on Block and Sublevel Caving*, Australian Centre for Geomechanics, Perth, pp. 313-322, https://doi.org/10.36487/ACG_rep/1815_21_Castro

Diering, T 2000, 'PC-BC: A block cave design and draw control system', *Proceedings of MassMin 2000*, The Australasian Institute of Mining and Metallurgy, Brisbane pp. 469–484.

Fuenzalida, MA, Pierce, ME & Katsaga, T 2018, 'REBOP–FLAC3D hybrid approach to cave modelling', in Y Potvin & J Jakubec (eds), *Caving 2018: Proceedings of the Fourth International Symposium on Block and Sublevel Caving*, Australian Centre for Geomechanics, Perth, pp. 297–312, https://doi.org/10.36487/ACG_rep/1815_20_Pierce

Ghazvinian, E, Fuenzalida, M, Orrego, C & Pierce, M 2020a, 'Back analysis of cave propagation and subsidence at Cadia East Mine', in R Castro, F Báez & K Suzuki (eds), *MassMin 2020: Proceedings of the Eighth International Conference & Exhibition on Mass Mining*, University of Chile, Santiago, pp. 535-550, https://doi.org/10.36487/ACG_repo/2063_36

Ghazvinian, E, Garza-Cruz, T, Bouzeran, L, Fuenzalida, M, Cheng, Z, Cancino, C & Pierce, M 2020b, 'Theory and implementation of the Itasca constitutive model for advanced strain softening (IMASS)', in *Proceedings of the International Conference on Mass Mining (MassMin 2020)*, Santiago, Chile, pp. 451–461.

Gibson, WH 2014, 'Stochastic models for gravity flow: numerical considerations', *Proceedings of the Third International Symposium on Block and Sublevel Caving,* Universidad de Chile, Santiago.

Gómez, R & Castro, R 2022, 'Stress modelling using cellular automata for block caving applications', *International Journal of Rock Mechanics and Mining Sciences*, vol. 154, https://doi.org/10.1016/j.ijrmms.2022.105124

Hebert, Y & Sharrock, G 2018, 'Three-dimensional simulation of cave initiation, propagation and surface subsidence using a coupled finite difference–cellular automata solution', in Y Potvin & J Jakubec (eds), *Caving 2018: Proceedings of the Fourth International Symposium on Block and Sublevel Caving*, Australian Centre for Geomechanics, Perth, pp. 151–166, https://doi.org/10.36487/ACG_rep/1815_09_Hebert

Itasca 2026, *MassFlow documentation, coupling example*, https://docs.itascacg.com/itasca920/massflow/enginemassflow/doc/manual/massflow_manual/massflow_examples/massflow_coupling.html?node7502#mining

Janssen, HA 1895, 'Versuche über Getreidedruck in Silozellen', *Zeitschrift des Vereines deutscher Ingenieure*, vol. 39, no. 1045.

Lorig, L 2000, *The role of numerical modelling in assessing caveability*, report to the International Caving Study, Itasca Consulting Group Inc., Minneapolis.

Pierce, M 2010, *A model for gravity flow of fragmented rock in block caving mines*, PhD thesis, The University of Queensland, Brisbane.

Power, GR & Campbell, AD 2016, 'Modelling of real time marker data to improve operational recovery in SLC mines', *MassMin 2016, Proceedings of the Seventh International Conference and Exhibition on Mass Mining*, The Australasian Institute of Mining and Metallurgy, Melbourne.

Sainsbury, BA 2012, *A model for cave propagation and subsidence assessment in jointed rock masses*, PhD thesis, The University of New South Wales, Sydney.

Sharrock, GB, Beck, DA, Capes, GW & Brunton, ID 2012, 'Applying coupled Newtonian cellular automata–discontinuum finite element models to simulate propagation of Ridgeway Deeps block cave', *Proceedings of MassMin 2012*, Canadian Institute of Mining, Metallurgy and Petroleum, Westmount.